

This is a repository copy of *The ice-free topography of Svalbard*.

White Rose Research Online URL for this paper:

<https://eprints.whiterose.ac.uk/id/eprint/138277/>

Version: Published Version

Article:

Fürst, Johannes, Navarro, Francisco, Gillet-Chaulet, Fabien et al. (23 more authors)
(2018) The ice-free topography of Svalbard. *Geophysical Research Letters*. ISSN: 0094-8276

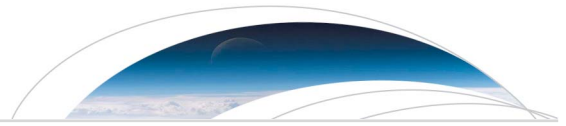
<https://doi.org/10.1029/2018GL079734>

Reuse

Items deposited in White Rose Research Online are protected by copyright, with all rights reserved unless indicated otherwise. They may be downloaded and/or printed for private study, or other acts as permitted by national copyright laws. The publisher or other rights holders may allow further reproduction and re-use of the full text version. This is indicated by the licence information on the White Rose Research Online record for the item.

Takedown

If you consider content in White Rose Research Online to be in breach of UK law, please notify us by emailing eprints@whiterose.ac.uk including the URL of the record and the reason for the withdrawal request.



Geophysical Research Letters

RESEARCH LETTER

10.1029/2018GL079734

Special Section:

The Arctic: An AGU Joint
Special Collection

Key Points:

- The presented glacier thickness map for Svalbard is informed by a comprehensive compilation of field measurements
- Robust numbers for the calving front thickness are key for estimating sea-level relevant ice discharge
- Thickness values are complemented by an associated error estimate map

Supporting Information:

- Supporting Information S1
- Figure S1
- Figure S2
- Figure S3
- Figure S4
- Figure S5

Correspondence to:

J. J. Fürst,
johannes.fuerst@fau.de

Citation:

Fürst, J. J., Navarro, F., Gillet-Chaulet, F., Huss, M., Moholdt, G., Fettweis, X., et al. (2018). The ice-free topography of Svalbard. *Geophysical Research Letters*, 45. <https://doi.org/10.1029/2018GL079734>

Received 24 JUL 2018

Accepted 3 OCT 2018

Accepted article online 9 OCT 2018

The Ice-Free Topography of Svalbard

Johannes J. Fürst¹ , Francisco Navarro² , Fabien Gillet-Chaulet^{3,4}, Matthias Huss^{5,6} , Geir Moholdt⁷, Xavier Fettweis⁸ , Charlotte Lang⁸, Thorsten Seehaus¹ , Songtao Ai⁹ , Toby J. Benham¹⁰, Douglas I. Benn¹¹ , Helgi Björnsson¹², Julian A. Dowdeswell¹⁰, Mariusz Grabiec¹³, Jack Kohler⁷ , Ivan Lavrentiev¹⁴, Katrin Lindbäck⁷ , Kjetil Melvold^{1,5,15}, Rickard Pettersson¹⁶ , David Rippin¹⁷ , Albane Saintenoy¹⁸, Sánchez-Gómez² , Thomas V. Schuler^{19,20} , Heïdi Sevestre¹¹ , Evgeny Vasilenko²¹, and Matthias H. Braun¹

¹Institute of Geography, University of Erlangen-Nuremberg, Erlangen, Germany, ²Departamento de Matemática Aplicada a las Tecnologías de la Información y las Comunicaciones, ETSI de Telecomunicación, Universidad Politécnica de Madrid, Madrid, Spain, ³Institut des Géosciences de l'Environnement, Grenoble, France, ⁴Université Grenoble Alpes, CNRS, IRD, Grenoble INP, IGE, Grenoble, France, ⁵Department of Geosciences, University of Fribourg, Fribourg, Switzerland, ⁶Laboratory of Hydraulics, Hydrology and Glaciology, ETH Zürich, Zurich, Switzerland, ⁷Norwegian Polar Institute, Fram Centre, Tromsø, Norway, ⁸Department of Geography, University of Liège, Liège, Belgium, ⁹Chinese Antarctic Center of Surveying and Mapping, Wuhan University, Wuhan, China, ¹⁰Scott Polar Research Institute, University of Cambridge, Cambridge, UK, ¹¹St Andrews Glaciology, School of Geography and Sustainable Development, University of St Andrews, St Andrews, UK, ¹²Institute of Earth Sciences, University of Iceland, Reykjavík, Iceland, ¹³Faculty of Earth Sciences, University of Silesia in Katowice, Katowice, Poland, ¹⁴Institute of Geography, Russian Academy of Sciences, Moscow, Russia, ¹⁵The Norwegian Water Resources and Energy Directorate (NVE), Oslo, Norway, ¹⁶Department of Earth Sciences, Geocentrum, Uppsala University, Uppsala, Sweden, ¹⁷Environment Department, University of York, York, UK, ¹⁸GEOPS, Université Paris-Sud, CNRS, Université Paris-Saclay, Orsay, France, ¹⁹Department of Geosciences, University of Oslo, Oslo, Norway, ²⁰Department of Arctic Geophysics, UNIS University Center on Svalbard, Longyearbyen, Norway, ²¹Institute of Industrial Research Akadempribo, Academy of Sciences of Uzbekistan, Tashkent, Uzbekistan

Abstract We present a first version of the Svalbard ice-free topography (SVIFT1.0) using a mass conserving approach for mapping glacier ice thickness. SVIFT1.0 is informed by more than 1 million point measurements, totalling more than 8,700 km of thickness profiles. SVIFT1.0 is publicly available and represents the geometric state around the year 2010. Our estimate for the total ice volume is 6,199 km³, equivalent to 1.5-cm sea level rise. The thickness map suggests that 13% of the glacierized area is grounded below sea level. A complementary map of error estimates comprises uncertainties in the thickness surveys as well as in other input variables. Aggregated error estimates are used to define a likely ice-volume range of 5,200–7,300 km³. The ice front thickness of marine-terminating glaciers is a key quantity for ice loss attribution because it controls the potential ice discharge by iceberg calving into the ocean. We find a mean ice front thickness of 135 m for the archipelago (likely range 123–158 m).

Plain Language Summary Svalbard is an archipelago in the Arctic, north of Norway, which is comparable in size to the New York metropolitan area. Roughly half of it is covered by glacier ice. Yet to this day, the ice volume stored in the many glaciers on Svalbard is not well known. Many attempts have been made to infer a total volume estimate, but results differ substantially. This surprises because of the long research activity in this area. A large record of more than 1 million thickness measurements exists, making Svalbard an ideal study area for the application of a state-of-the-art mapping approach for glacier ice thickness. The mapping approach computes an ice volume that will raise global sea level by more than half an inch if instantaneously melted. If spread over the metropolitan area, New York would be buried beneath a 100-m ice cover. The asset of this approach is that it provides not only a thickness map for each glacier on the archipelago but also an error map that defines the likely local thickness range. Finally, we provide the first well-informed estimate of the ice front thickness of all marine-terminating glaciers that loose icebergs to the ocean. The archipelago-wide mean ice front cliff is 135 m.

1. Introduction

Apart from the many glaciers that drain the two large ice sheets on Antarctica and Greenland, there are more than 200,000 other glaciers and ice caps (henceforth glaciers) worldwide (RGI6.0; RGI Consortium, 2017). For the large majority of these glaciers, no thickness measurements are available (Gärtner-Roer et al., 1981). In light of a warming climate and the associated glacier demise (Vaughan et al., 2013), a well-constrained quantification of the available ice volume is indispensable for reliable projections of the future glacier sea level contribution. A standing problem in glaciology is therefore to derive glacier ice volumes from other accessible surface information. A simple and robust approach is volume-area scaling (VAS), first introduced by Erasov (1968), substantiated by theoretic arguments (Bahr et al., 1997), and continuously refined further (Adhikari & Marshall, 2012; Bahr et al., 2015; Grinsted, 2013). VAS is thus a standard method to get a first estimate of regional-scale glacier ice volume. Yet two recent applications report a global glacier and ice cap volume of 139,510 and 209,973 km³ (Grinsted, 2013; Radić et al., 2014), which translate to 0.35 and 0.52 m sea level equivalent, respectively. The large difference is emblematic and reflects the generally poor knowledge of glacier ice thickness.

For Svalbard, ice thickness is relatively well known because of the long research activity comprising deep ice coring (overview in Kotlyakov et al., 2004), airborne radio-echo soundings (RESs; Dowdeswell & Bamber, 1995; Dowdeswell & Drewry, 1984; Dowdeswell et al., 1986; Macheret & Zhuravlev, 1982), and numerous ground-penetrating radar surveys (overview in ; Martín-Español et al., 2013). These records allowed a first tuning of VAS approaches against thickness measurements and their archipelago-wide application. Macheret et al. (1984) inferred a total ice volume of 7,567 km³. A series of updated VAS estimates followed: 6,988 km³ (H93, Hagen et al., 1993); 4,000 km³ (Ohmura, 2004); 10,260 km³ (RH10, Radić & Hock, 2010); 5,350 km³ (Grinsted, 2013); 9,089 km³ (Radić et al., 2014); and 6,746 km³ Martín-Español et al. (2015). The large spread is explained by the global scope of most of these studies. H93 and ME15 did focus only on Svalbard, and similar values are reported. Considering the elapsed time and current volume loss rates (Moholdt et al., 2010a; Nuth et al., 2010), the two estimates become almost identical.

A spatially resolved thickness field is necessary to attribute recent surface elevation changes either to surface mass balance (SMB) variations or to ice dynamic effects (Nuth et al., 2010). Moreover, the glacier thickness field is required to partition and attribute the annual ice loss of ~11 km³/year (Moholdt et al., 2010b; Nuth et al., 2010; Wouters et al., 2008) into its two main components, that is, ice discharge at the marine margins by ice-berg calving and SMB changes. The last archipelago-wide ice discharge estimate of ~7 km³/year (Błaszczyk et al., 2009) suffers from sparse thickness observations near the often inaccessible ice fronts, and it had to rely on the *historic* 100-m estimate of the mean frontal thickness, forwarded in Hagen et al. (2003). A great leap forward was the reconstruction approach by Farinotti et al. (2009), which forms the basis for a first world-wide reconstruction (HF12, Huss & Farinotti, 2012) providing thickness maps for all glaciers. On Svalbard, HF12 reports a total ice volume of 9,685 km³. After updating to RGI6.0, the HF12 approach gives a mean ice front thickness of 214 m, twice as large as the historic value. HF12 was calibrated with observations from 31 glaciers on Svalbard. The primary intention of their calibration was to provide a best volume estimate and not the reproduction of individual measurements.

Until now, the many ice thickness records on Svalbard have not been compiled into a single database. Here we aim at assimilating this exceptional record and produce a Svalbard map of glacier ice thickness. For this purpose, we apply an existing mass conservation approach (Fürst et al., 2017) to all glacierized areas accounting for surface velocities, SMB, glacier hypsometry, and changes therein.

2. Methods

Details of the two-step thickness reconstruction method employed here are presented in Fürst et al. (2017). Some further method adaptations are presented in the Text S1 in the supporting information (Carrivick et al., 2016; Lapazaran et al., 2016; Noël et al., 2016; Norwegian Polar Institute, 2014; Pinglot et al., 2001; Pinglot et al., 1999; Schutz et al., 2005; Wingham et al., 2006). The approach is primarily based on mass conservation and requires prior knowledge of source and sink terms in the glacier mass budget. Assuming incompressibility, the mass conservation is reformulated in terms of glacier ice thickness H .

$$\partial_t H + \nabla \cdot (\bar{\mathbf{u}}H) = \dot{b}_s \quad (1)$$

Here ∂_t and $\nabla \cdot$ denote the partial time derivative and the 2-D horizontal divergence operator, respectively. $\bar{\mathbf{u}}$ is the vertically averaged, horizontal velocity vector. The SMB \dot{b}_s comprises mass gain and loss terms at the upper glacier surface. The difference $\dot{b}_s - \partial_t H$ is referred to as the apparent mass balance.

In this formulation, we deliberately neglect any influence from internal and basal mass balance processes. To solve equation (1), we use the Elmer finite-element software developed at the Center for Science in Finland [http://www.csc.fi/elmer/CSC-IT\(CSC-IT\)](http://www.csc.fi/elmer/CSC-IT(CSC-IT)) and more specifically the mass conservation solver implemented in its glaciological extension Elmer/Ice (Gagliardini & Zwinger, 2008; Gagliardini et al., 2013; Gillet-Chaulet et al., 2012). For the modeling domain, a 2-D triangular-element mesh is generated using the open-source <http://gmsh.info/> Gmsh software (Geuzaine & Remacle, 2009). To avoid internal boundaries, the reconstruction is performed for glacier compounds by merging adjacent glacier outlines. Dependent on the compound area, the nominal resolution ranges from 25 to 300 m (Table S1).

A two-step approach is necessary because surface velocity measurements from satellite remote sensing are often not available over the entire glacierized area. Therefore, the first step requires no velocity information. Equation (1) is solved for the unknown ice flux $\mathbf{F} = \bar{\mathbf{u}}H$. Subsequently, \mathbf{F} is converted into ice thickness values assuming the shallow ice approximation (Hutter, 1983; Morland, 1986). The conversion comprises the free viscosity parameter (as defined in equation 7 in; Fürst et al., 2017), which is calibrated with thickness measurements (Table S1). In subregions where flow speeds exceed 100 m/year the thickness field is updated in a second step, accounting for the observed flow routing. For this step, we assume equality between surface and vertical mean velocities. In these subregions, the thickness update is laterally constrained by first-step thickness values. In both steps, marine ice fronts are treated as free boundaries. Moreover, equation (1) is cast as a minimization problem using a cost function that penalizes negative solutions, high spatial variability, and the mismatch to observations.

The inferred thickness field is provided together with an error estimate map, based on a formal propagation of input uncertainties (Morlighem et al., 2011). In Fürst et al. (2017), uncertainty values of input fields are given as well as details of the error propagation for both steps. An assessment of the error estimates on several test geometries from Svalbard showed that in a median sense, error estimates tend to overestimate actual mismatch values between modeled and withheld thickness measurements (Fürst et al., 2017).

3. Input Data

In the following, we present a brief overview of the input fields. A more comprehensive description is provided in Text S2. (Ai et al., 2014; Bamber & Dowdeswell, 1990; Björnsson et al., 1996; Dowdeswell et al., 1984; Drewry & Liestøl, 1985; Fujii et al., 1990; Grabiec et al., 2012; Jania et al., 1996; Kotlyakov, 1985; Lindbäck et al., 2018; Melvold & Schuler, 2008; Melvold et al., 2003; Navarro et al., 2005, 2014, 2015; Saintenoy et al., 2013; Schuler et al., 2005; van Pelt et al., 2013; Vasilenko et al., 2009; Zagorodnov & Arkipov, 1990; Zagorodnov & Samoilov, 1982; Zagorodnov & Zotikov, 1981). The glacier surface geometry is based on an archipelago-wide reference digital elevation model (DEM), which was primarily inferred from airborne stereo-imagery collected between 2008 and 2012. The center of this time period 2010 defines the time stamp of the thickness map product. Elevation changes are calculated by differencing the reference DEM with another composite DEM based on photogrammetric information from the 1990s and processed satellite imagery (Moholdt & Kääb, 2012; Nuth et al., 2010). The glacier outlines are taken from Nuth et al. (2013), representing the period 2002–2010. These outlines also entered the RGI. Despite the ice geometry and changes therein, the reconstruction requires information on the SMB. An archipelago-wide product was computed for the period 1979–2013 with the regional climate model Modèle Atmosphérique Régional (Lang et al., 2015). The original setup was recently rerun at 3.75-km resolution, and results were subsequently downscaled spatially and averaged for the period 1990–2010 (Franco et al., 2012). The downscaling is necessary to obtain distributed SMB information over all glaciers also for smaller geometries. Surface velocities (Figure S1) were determined by intensity offset tracking using consecutive image pairs of Sentinel 1 acquired in the period January 2015 and September 2016 (Seehaus et al., 2016; Strozzi et al., 2002).

In this study, we considered 1,002,684 individual RES measurements from airborne and ground-based campaigns (overview in Figure S2 and Table S2). These campaigns add up to a total RES profile length of 8,737 km. The RES measurements are completed by information from 13 deep ice cores and 112 boreholes (Table S3).

On account of the target map resolution of 100 m and the spatial correlation characteristics of thickness measurements, the data were subsampled to 50 m. Since thickness measurements were collected between 1980 and 2016, a prior homogenization is required, correcting the values by elevation changes since acquisition with respect to the reference DEM.

4. Results

The reconstructed fields for ice thickness represent the state around 2010 (Figure 1a). Together with the basal topography (Figure S3), the thickness field is analyzed on a regular raster with 100-m spacing in accordance with the downsampled reference DEM. Covering all of the 1,668 glacier units on the archipelago, we find a total ice volume of $6,199 \text{ km}^3$ (Table 1), equal to 1.5-cm sea level equivalent. Half of the volume is stored in the two ice caps on Nordaustlandet (Austfonna: $2,658 \text{ km}^3$; Vestfonna: 513 km^3). The many glaciers on Spitsbergen comprise a slightly smaller volume of $2,532 \text{ km}^3$. The thickness map is provided together with an error estimate field (Figure S4 and section 2), which indicates spatial differences in the reliability of the reconstruction. Error values are systematically larger over the ice caps on Nordaustlandet, Edgeøya, Barentsøya, and Kvitøya as compared to the ice fields on Spitsbergen. There are three reasons for this difference. First, a multitude of nunataks (or elongated crests) protrudes through the ice cover on Spitsbergen, and error estimates naturally decrease in their vicinity. For the ice caps, only a few nunataks exist. Second, large portions of these ice caps were only surveyed in the 1980s by airborne RES campaigns with large measurement errors mainly stemming from pre-GPS navigation. Third, in the absence of measurements, the method has difficulties to efficiently constrain errors over the flat topography over the interior of ice caps (Fürst et al., 2017).

In Fürst et al. (2017), it has been shown that median error values from all measurement locations exceed the median of the actual mismatch to the observed ice thickness. We assume that this aggregate overestimation can be transferred to unsurveyed terrain. Normalizing the glacier-wide median error estimates with respect to mean glacier thicknesses, we find that for more than 50% of the glacierized area, the uncertainty in mean glacier thickness falls below 11% (Figure 1b). For 90% of the glacier area, this uncertainty is smaller than 29%. These numbers increase to 12% and 52%, if we use arithmetic means instead of medians. In terms of mean values, large error values get higher weights, and more conservative error intervals are found. Henceforth, aggregate error intervals are defined in the arithmetic mean sense and used as likely error ranges for ice-volume and average ice thickness values. For the ice volume on Svalbard, the likely range is $5,210\text{--}7,309 \text{ km}^3$.

The ice front thickness of marine-terminating glaciers is of high interest in terms of possible implications for sea level change, as it sets a natural limit on annual ice loss rates by iceberg calving. We find an archipelago-wide frontal thickness average of 135 m with a likely range of 123 to 158 m (Table 1). For glaciers with a dense measurement network, frontal thickness values can be well constrained. This is the case for Kronbreen, Tunabreen, and Basin 3 of Austfonna, where maximum error bounds lie within 10% of the mean value. For Hansbreen and Paierlbreen, frontal areas are densely surveyed, and we attain accuracies of the mean value of 4 and 8 m, respectively. For glaciers with limited, or no ground truth, such as Monacobreen and Nathorstbreen, the likely range exceeds 100 m.

On Spitsbergen the inferred bedrock topography is a complex system of interconnected valleys (Figure S3). On Nordaustlandet, there is not such a clear partitioning of the landscape into well-imprinted valley systems either in the ice-free areas or beneath the ice caps. For the whole of Svalbard, we find that 13% of the glacierized area is grounded below sea level. Our results support the speculation that Sørkapp is a potential island separated by an ocean channel beneath Hornbreen and Hambergbreen (Grabiec et al., 2018). At present, the shallowest portion is covered by 180-m-thick ice. Error magnitudes (Figure S4) are well constrained by nearby measurements, and they compare to the inferred bathymetric depth of 3–20 m in this area.

5. Discussion

Our total volume estimate of $6,199 \text{ km}^3$ is bracketed by previous estimates ranging from 4,000 to $10,000 \text{ km}^3$ (see section 1). However, many of these estimates do not fall into the likely range ($\sim 5,300\text{--}7,300 \text{ km}^3$; Table 1) that is determined by the aggregated errors. Even within these bounds, differences are still important, considering current loss rates on Spitsbergen of $\sim 100 \text{ km}^3$ per decade (Moholdt et al., 2010a; Nuth et al., 2010). In fact, only the two VAS approaches with exclusive focus on Svalbard (H93 and ME15) report comparable ice volumes. In terms of the regional volume distribution, it was often speculated that most ice resides within the

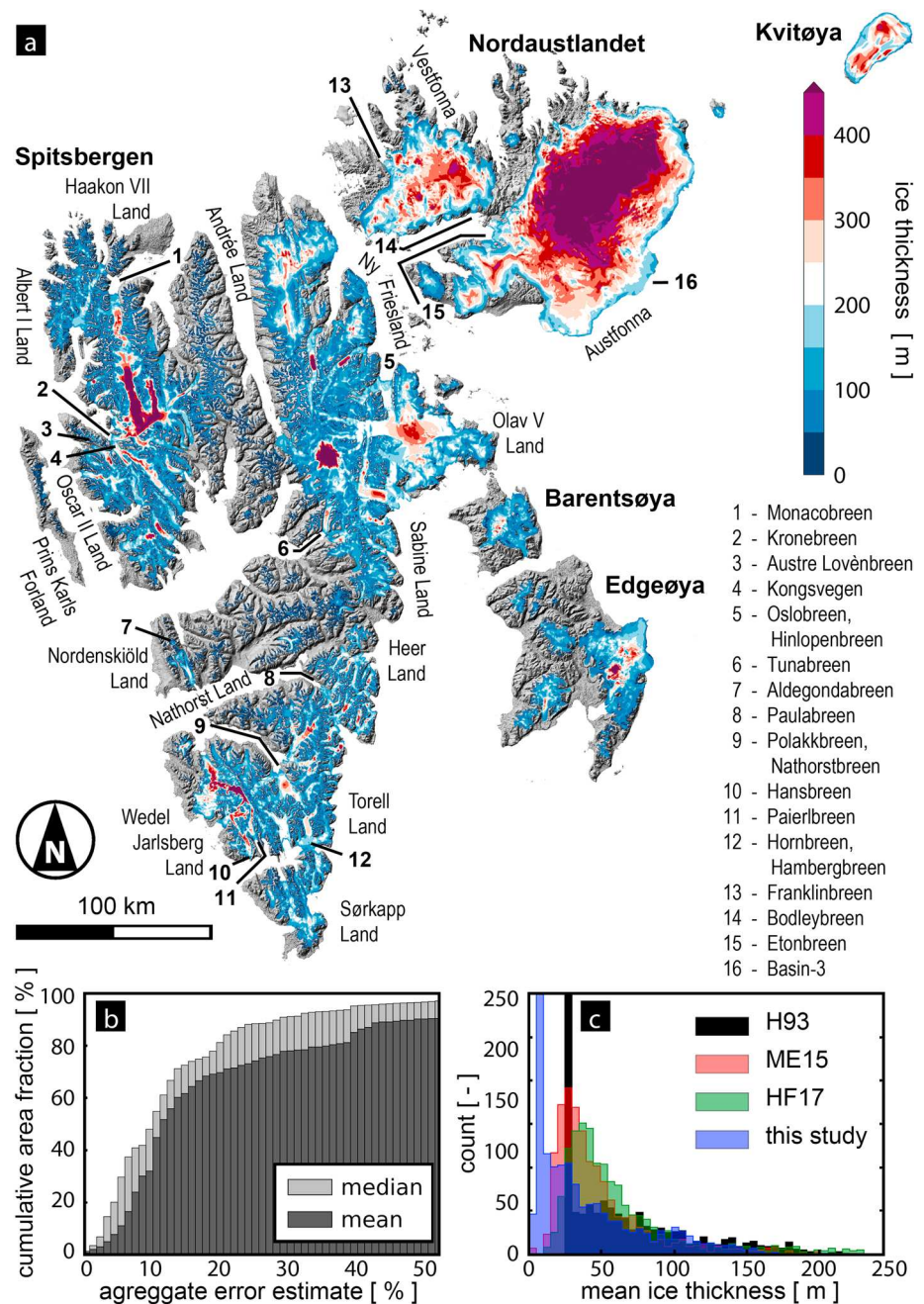


Figure 1. (a) Svalbard ice thickness map. More than 1 million individual measurements were considered in the underlying reconstruction approach (Füerst et al., 2017). Island names of the archipelago are given in bold. Regular font is used for region names and prominent glaciers (numbered list). Inset (b) shows the cumulative area fraction in ascending order of the aggregate error estimate per glacier unit. The inset histogram (c) shows the distribution of the mean glacier thickness in 5-m bins. Mean thickness values for H93 (Hagen et al., 1993) and ME15 (Martín-Español et al., 2015) were updated with the 2002–2010 inventory (Nuth et al., 2013) using the VAS formulas in the respective publications. H93 uses a minimum mean thickness of 25 m for glaciers smaller than 1 km². HF17 refers to a recent update of HF12 (Huss & Farinotti, 2012) relying on the RGL6.0 (see map in Figure S5).

Table 1
Characteristic Quantities of SVIFT1.0

Regional breakdown	H93	ME15	HF17	SVIFT 1.0	
Ice volume (km ³)					
Svalbard	6,649 (6,988)	6,849 (6,746)	8,123	6,199	(7,309) (5,210)
By region					
Spitsbergen	3,444 (3,899)	3,377 (—)	4,057	2,532	(29,121) (2,184)
Nordautlandet	2,654 (2,444)	3,001 (3,001)	3,465	3,221	(3,743) (2,742)
Edgeøya	309, (376)	271 (—)	347	236	(357) (139)
Barentsøya	93 (98)	69 (—)	106	58	(75) (41)
Kvitøya	124 (170)	130 (—)	148	153	(213) (104)
Area grounded below sea level (km ²)					
Svalbard	—	—	7,391	4,275	(6,291) (2,818)
Mean ice thickness (m)					
Svalbard	197 (191)	203 (200)	240	184	(216) (154)
Mean calving front thickness (m)					
Svalbard	—	—	214	135	(158) (123)
By glacier					
Monacobreen	—	—	331	97	(466) (50)
Kronebreen and Kongsvegen	—	—	157	124	(137) (112)
Hinlopenbreen and Oslobreen	—	—	103	121	(133) (110)
Tunabreen	—	—	208	120	(126) (114)
Paulabreen	—	—	129	117	(150) (84)
Nathorstbreen and Polakkbreen	—	—	104	116	(164) (72)
Hansbreen	—	—	142	108	(112) (104)
Paierlbreen	—	—	140	86	(94) (80)
Franklinbreen	—	—	175	141	(173) (125)
Bodleybreen	—	—	100	110	(145) (74)
Etonbreen	—	—	240	157	(182) (132)
Basin 3, Austfonna	—	—	329	147	(171) (122)

Note. Values are compared to volume-area scaling (VAS) results from Hagen et al. (1993; H93) and Martín-Español et al. (2015; ME15) as well as the updated HF17 map of distributed thickness values from Huss and Farinotti (2012). VAS values are recomputed for the Nuth et al. (2013) inventory (for H93 and ME15, values in parentheses are from the original study). Calving front thicknesses are averaged within a 1-km band along the marine glacier margin. The marine margin adds up to 1,541 km on the archipelago. Bold numbers highlight values that exceed the error range from this study (subscript and superscript values in parentheses). Error ranges are asymmetric because thickness values cannot be negative.

glaciers of Spitsbergen. This speculation was substantiated by the recent distributed ice thickness reconstruction (HF12; Huss & Farinotti, 2012). Together with ME15, we find a more balanced situation with a tendency for more ice on Nordautlandet. For the ice cap on Kvitøya, a good volume agreement is achieved (Table 1). Previous ice-volume estimates for Barentsøya and Edgeøya need downward correction because, there, our reconstruction is informed by early airborne campaigns (Table S2).

The HF12 approach was rerun for the RGI6.0 (referred to as HF17), and the total ice volume was updated to 8,123 km³. This updated value remains somewhat larger than our estimate and exceeds the inferred error bounds (Table 1). In general, glaciers tend to be thicker in HF17 (Figures 1c and S5). For Vestfonna, Aldegondabreen, and Austre Lovénbreen, we consider the same thickness measurements as HF12 (and thus HF17)

in their global calibration. For the latter two glaciers, we find mean thickness values of 60 and 78 m, respectively. This is in reasonable agreement with the 69 and 68 m in HF17. Ice cap thickness distributions are more challenging to infer because of gentle surface slopes over most of the ice-covered area. Consequently, the mismatch on Vestfonna is higher with 275 m as compared to our 227 m. Our estimate is well constrained by measurements (Figure S2).

In 1983, a large airborne RES campaign targeted the two ice caps on Nordaustlandet (Dowdeswell, 1986). Data gaps along the Vestfonna ice divide were filled by additional GPR measurements in 2008–2009 (Pettersson et al., 2011). The good spatial coverage of these data sets justified a direct interpolation, and an average thickness value of 309 m was reported for Austfonna (Dowdeswell et al., 2008) and 186 m for Vestfonna (Pettersson et al., 2011). Here we largely rely on the same measurements, and we find somewhat higher values of 329 and 227 m, respectively. On Austfonna, about 4 m of this difference is explained by the widespread positive surface elevation changes between 1996 and 2011. On Vestfonna, however, elevation changes indicate mass loss in the same period. There, we infer a thicker ice cover in unsurveyed areas around the land-terminating margin and along a few outlet glaciers (also see Fürst et al., 2017). Moreover, Pettersson et al. (2011) reported that 5% of the Vestfonna bed lies below present sea level. This value is incompatible with our estimate of 13%, considering the likely range of 6% to 31%. The upper bound of the area fraction grounded below sea level for Vestfonna matches the 30% from the updated HF17 reconstruction. For Austfonna, HF17 finds that 36% of the bed lie below sea level, exceeding the upper bound of 32% found for the likely range (central estimate 24%).

A glacier classification by area allows a direct comparison of mean thicknesses with earlier VAS approaches (Figure 1c). The distribution, we find, agrees well with the H93 estimates. The match is more moderate in the thickness range of 125–175 m, where H93 reported more glaciers. H93 employed a lower bound of 25 m. In the range between 25 and 75 m, ME15 and HF17 show a different distribution with almost twice as many glaciers with respect to our distribution. In terms of the H93 formulation, this range comprises glaciers up to $\sim 5 \text{ km}^2$. In our reconstruction, most of these glaciers are larger than 1 km^2 , for which our reconstruction is constrained by measurements (Table S1). In contrast to all previous approaches, we find a large number of glaciers with thickness values below 15 m. We feel not very confident about these small values, because they mostly appear on glaciers smaller than 1 km^2 . In this area class, direct measurements were only available on one land-terminating glacier (Table S1). Moreover, the SMB downscaling reaches its limits for these small geometries. After subtracting $\partial_t H$, the resultant apparent mass balance often gives not much rise to glacier motion, and inferred thickness values remain small. If we use 25 m as a lower limit on glacier mean thickness (affecting a 2.1% area fraction), the total volume estimate increases by 6 km^3 or 0.1%.

From the 1668 glacier units on Svalbard, 197 are marine terminating. These few glaciers drain 69% of the glacierized area and thereby access 80% ($4,977 \text{ km}^3$) of the stored ice volume. Though volume magnitudes differ, HF17 confirms a 79% fraction. In terms of sea level relevant ice discharge, the main unknown is the ice front thickness of marine-terminating glaciers. This thickness value is a key characteristic of mass conserving reconstruction approaches, because it comprises and reflects the cumulative effect of all input uncertainties. HF17 presents an archipelago-mean estimate of 214 m, well beyond our likely range (Table 1). A reason is again the global scope of HF17, which could only consider marine termination as a region-specific perturbation on the equilibrium line altitude (Huss & Farinotti, 2012). The historic estimate of the archipelago-wide ice front thickness is 100 m (Hagen et al., 1993). This estimate was not intended to precisely pin down the exact value, but it gives a valuable orientation. As this value was used for the last Svalbard-wide ice discharge estimate of $7 \text{ km}^3/\text{year}$ (Błaszczyk et al., 2009), we expect a nonnegligible upward correction. On a glacier-to-glacier basis, mean ice front thickness values in HF17 often exceed the upper error bound. For Basin 3 on Austfonna, which is well surveyed, HF17 finds a more than twice as thick mean ice front. On Monacobreen in northern Spitsbergen, a factor 3 is reached, still within the error range. The HF17 reconstruction also suggests that 22% of the glacierized area is grounded below sea level. We can only confirm 13% with an upper bound of 21%. Again, these differences are partly explained by the ad hoc perturbation strategy for marine-terminating glacier in HF12.

6. Conclusions

Despite other existing ice-volume estimates on Svalbard (see section 1) and available glacier thickness maps (Huss & Farinotti, 2012), the presented map of the Svalbard ice-free topography version 1.0 (SVIFT1.0) is novel

in two aspects. First, an abundant record of more than 1 million individual thickness measurements was compiled, and observations are imprinted in the thickness map. In this way, the reliability is increased, making the map a valuable and long-anticipated product required for ice flow model application on Svalbard. Second, an associated map of error estimates is provided, which informs on spatial differences in reliability. Aggregated error values are further used to define likely ranges for mean glacier thickness, for calving front thickness as well as for glacier volumes.

Our volume estimate is expedient, given the good agreement with two independent estimates from regionally calibrated VAS approaches (Hagen et al., 1993; Martín-Español et al., 2015). Relative differences of less than 10% are rather precise, considering the large range of existing VAS estimates (4,000 to 10,000 km³). The consistency also indicates that VAS approaches clearly benefit from ground-truth data. However, the thickness distributions reveal clear differences in certain glacier area classes. These discrepancies require further investigation and might help to refine the methodology.

The large record of thickness measurements, which entered SVIFT1.0, enables a first well-informed estimate of the calving front thickness of marine-terminating glaciers. The existing HF17 map is of inferior quality in this aspect because significantly less thickness measurements were used and because an ad hoc perturbation strategy was applied to generate nonzero calving fluxes (Huss & Farinotti, 2012). The knowledge of the ice front thickness is key for a reliable quantification of the sea level relevant ice discharge and thus total mass loss attribution.

Acknowledgments

This study received primary funding from the German Research Foundation (DFG) within the Svalbard-iFLOWbed project, Grant FU1032/1-1. Further collaborators and funding organizations are acknowledged in Text S3. SVIFT1.0 data (<https://doi.org/10.21334/npolar.2018.57fd0db4>) and all used thickness measurements (<https://doi.org/10.5904/wgms-glathida-2016-07>) are publicly available. The authors declare that they have no conflict of interest.

References

- Adhikari, S., & Marshall, S. (2012). Glacier volume-area relation for high-order mechanics and transient glacier states. *Geophysical Research Letters*, 39, L16505. <https://doi.org/10.1029/2012GL052712>
- Ai, S., Wang, Z., Dongchen, E., Holm  n, K., Tan, Z., Zhou, C., & Sun, W. (2014). Topography, ice thickness and ice volume of the glacier Pedersenbreen in Svalbard, using GPR and GPS. *Polar Research*, 33(1), 18533. <https://doi.org/10.3402/polar.v33.18533>
- Bahr, D. B., Meier, M. F., & Peckham, S. D. (1997). The physical basis of glacier volume-area scaling. *Journal of Geophysical Research*, 102(B9), 20,355–20,362. <https://doi.org/10.1029/97JB01696>
- Bahr, D., Pfeffer, W., & Kaser, G. (2015). A review of volume-area scaling of glaciers. *Reviews of Geophysics*, 53, 95–140. <https://doi.org/10.1002/2014RG000470>
- Bamber, J., & Dowdeswell, J. (1990). Remote-sensing studies of Kvit  j  kulen, an ice cap on Kvit  ya, north-east Svalbard. *Journal of Glaciology*, 36(122), 75–81. <https://doi.org/10.1017/S002214300000558X>
- Bj  rnsson, H., Gjessing, Y., Hamran, S., Hagen, J., Liest  l, O., P  lsson, F., & Erlingsson, B. (1996). The thermal regime of sub-polar glaciers mapped by multi-frequency radio-echo sounding. *Journal of Glaciology*, 42(140), 23–32.
- B  larczyk, M., Jania, J., & Hagen, J. (2009). Tidewater glaciers of Svalbard: Recent changes and estimates of calving fluxes. *Polish Polar Research*, 30(2), 85–142.
- Carrivick, J., Davies, B., James, W., Quincey, D., & Glasser, N. (2016). Distributed ice thickness and glacier volume in southern South America. *Global and Planetary Change*, 146, 122–132. <https://doi.org/10.1016/j.gloplacha.2016.09.010>
- Dowdeswell, J. (1986). Drainage-basin characteristics of Nordaustlandet ice caps, Svalbard. *Journal of Glaciology*, 32, 31–38.
- Dowdeswell, J., & Bamber, J. (1995). On the glaciology of Edge  ya and Barents  ya, Svalbard. *Polar Research*, 14(2), 105–122.
- Dowdeswell, J., Benham, T., Strozzi, T., & Hagen, J. (2008). Iceberg calving flux and mass balance of the Austfonna ice cap on Nordaustlandet, Svalbard. *Journal of Geophysical Research*, 113, F03022. <https://doi.org/10.1029/2007JF000905>
- Dowdeswell, J., & Drewry, D. (1984). Airborne radio echo sounding of sub-polar glaciers in Spitsbergen. *Norwegian Polar Institute Skrifter*, 182, 44. Retrieved from <https://brage.bibsys.no/xmlui/handle/11250/173505?show=full>
- Dowdeswell, J., Drewry, D., Cooper, A., & Gorman, M. (1986). Digital mapping of the Nordaustlandet ice caps from airborne geophysical investigations. *Annals of Glaciology*, 8, 51–58. <https://doi.org/10.1175/2010JCLI3656.1>
- Dowdeswell, J., Drewry, D., Liest  l, O., & Orheim, O. (1984). Radio echo-sounding of Spitsbergen glaciers: Problems in the interpretation of layer and bottom returns. *Journal of Glaciology*, 30(104), 16–21.
- Drewry, D., & Liest  l, O. (1985). Glaciological investigations of surging ice caps in Nordaustlandet. *Polar Record*, 22, 359–378.
- Erasov, N. (1968). IMethod to determine the volume of mountain glaciers. *Data of Glaciological Studies*, 14, 307–308.
- Farinotti, D., Huss, M., Bauder, A., Funk, M., & Truffer, M. (2009). A method to estimate the ice volume and ice-thickness distribution of alpine glaciers. *Journal of Glaciology*, 55(191), 422–430. <https://doi.org/10.3189/002214309788816759>
- Franco, B., Fettweis, X., Lang, C., & Erpicum, M. (2012). Impact of spatial resolution on the modelling of the Greenland ice sheet surface mass balance between 1990–2010, using the regional climate model MAR. *The Cryosphere*, 6(3), 695–711. <https://doi.org/10.5194/tc-6-695-2012>
- Fujii, Y., Kamiyama, K., Kawamura, T., Kameda, T., Izumi, K., Satow, K., et al. (1990). 6000-year climate records in an ice core from the H  ghetta ice dome in northern Spitsbergen. *Annals of Glaciology*, 14, 85–89.
- F  rst, J., Gillet-Chaulet, F., Benham, T., Dowdeswell, J., Grabiec, M., Navarro, F., et al. (2017). Application of a two-step approach for mapping ice thickness to various glacier types on Svalbard. *The Cryosphere Discussions*, 2017, 1–43. <https://doi.org/10.5194/tc-2017-30>
- Gagliardini, O., & Zwinger, T. (2008). The ISMIP-HOM benchmark experiments performed using the finite-element code Elmer. *The Cryosphere*, 2(1), 67–76. <https://doi.org/10.5194/tc-2-67-2008>
- Gagliardini, O., Zwinger, T., Gillet-Chaulet, F., Durand, G., Favier, L., de Fleurian, B., et al. (2013). Capabilities and performance of Elmer/Ice, a new-generation ice sheet model. *Geophysical Model Development*, 6, 1299–1318. <https://doi.org/10.5194/gmd-6-1299-2013>
- G  rtner-Roer, Andreassen, L., et al. (Eds.) (2016). *WGMS (2016): Glacier thickness database 2.0 Edited by G  rtner-Roer, Andreassen, L., Bjerre, E., Farinotti, D., Fischer, A., Fischer, M., Helfricht, K., Huss, M., Knecht, T., Kutuzov, S., Landmann, J., Lavrentiev, I., Li, H., Li, Z., Machguth, H., Naegeli, K., Navarro, F., Rabatel, A., Stentoft, P., & Zemp, M.* Zurich, Switzerland: World Glacier Monitoring Service. <https://doi.org/10.5904/wgms-glathida-2016-07>

- Geuzaine, C., & Remacle, J. (2009). Gmsh: A three-dimensional finite element mesh generator with built-in pre- and post-processing facilities. *International Journal for Numerical Methods in Engineering*, 79(11), 1309–1331.
- Gillet-Chaulet, F., Gagliardini, O., Seddik, H., Nodet, M., Durand, G., Ritz, C., et al. (2012). Greenland ice sheet contribution to sea-level rise from a new-generation ice-sheet model. *The Cryosphere*, 6(6), 1561–1576. <https://doi.org/10.5194/tc-6-1561-2012>
- Grabiec, M., Ignatiuk, D., Jania, J., Moskalik, M., Glowacki, P., Błaszczyk, M., et al. (2018). Coast formation in an Arctic area due to glacier surge and retreat: The Hornbreen-Hambergreen case from Spitsbergen. *Earth Surface Processes and Landforms*, 43(2), 387–400. <https://doi.org/10.1002/esp.4251>
- Grabiec, M., Jania, J., Puczek, D., Kolondra, L., & Budzik, T. (2012). Surface and bed morphology of Hansbreen, a tidewater glacier in Spitsbergen. *Polish Polar Research*, 33(2), 111–138. <https://doi.org/10.2478/v10183-012-0010-7>
- Grinsted, A. (2013). An estimate of global glacier volume. *The Cryosphere*, 7, 141–151. <https://doi.org/10.5194/tc-7-141-2013>
- Hagen, J., Liestøl, O., Roland, E., & Jørgensen, T. (1993). Glacier Atlas of Svalbard and Jan Mayen. *Norsk Polarinstitutt Meddelelser*, 129, 1–141.
- Hagen, J., Melvold, K., Pinglot, F., & Dowdeswell, J. (2003). On the net mass balance of the glaciers and ice caps in Svalbard, Norwegian Arctic. *Arctic, Antarctic, and Alpine Research*, 35(2), 264–270.
- Huss, M., & Farinotti, D. (2012). Distributed ice thickness and volume of all glaciers around the globe. *Journal of Geophysical Research*, 117, 10. <https://doi.org/10.1029/2012JF002523>
- Hutter, K. (1983). *Theoretical glaciology. Material science of ice and the mechanics of glaciers and ice sheets*. Dordrecht, Boston, Tokyo, Japan, and Hingham: Publishing Company/Tokyo, Terra Scientific Publishing Company.
- Jania, J., Mochnacki, D., & Gądek, B. (1996). The thermal structure of Hansbreen, a tidewater glacier in southern Spitsbergen, Svalbard. *Polar Research*, 15(1), 53–66.
- Kotlyakov, V. (Ed.) (1985). *Glaciology of Spitsbergen* Edited by Kotlyakov, V., pp. 200. Nauka, Moscow.
- Kotlyakov, V., Arkhipov, S., Henderson, K., & Nagornov, O. (2004). Deep drilling of glaciers in Eurasian Arctic as a source of paleoclimatic records. *Quaternary Science Reviews*, 23(11), 1371–1390. <https://doi.org/10.1016/j.quascirev.2003.12.013>
- Lang, C., Fettweis, X., & Ericum, M. (2015). Stable climate and surface mass balance in Svalbard over 1979–2013 despite the Arctic warming. *The Cryosphere*, 9(1), 83–101. <https://doi.org/10.5194/tc-9-83-2015>
- Lapazaran, J., Otero, J., Martín-Español, A., & Navarro, F. (2016). On the errors involved in ice-thickness estimates I: Ground-penetrating radar measurement errors. *Journal of Glaciology*, 62(236), 1008–1020. <https://doi.org/10.1017/jog.2016.93>
- Lindbäck, K., Kohler, J., Pettersson, R., Nuth, C., Langley, K., Messerli, A., et al. (2018). Subglacial topography, ice thickness, and bathymetry of Kongsfjorden, northwestern Svalbard. *Earth System Science Data Discussions*, 2018(in review), 1–19. <https://doi.org/10.5194/essd-2018-37>
- Macheret, Y., & Zhuravlev, A. (1982). Radio echo-sounding of Svalbard glaciers. *Journal of Glaciology*, 28(99), 295–314.
- Macheret, Y., Zhuravlev, A., & Bobrova, L. (1984). Tolshchina, podlednyy rel'yef i ob'yem lednikov Shpitsbergena po dannym radiozondirovaniya [Thickness, subglacial relief and volume of Svalbard glaciers from radio echo-sounding data]. *Materialy Glyatsiologicheskikh Issledovaniy, Khronika, Obsuzhdeniya*, 51, 49–63.
- Martín-Español, A., Navarro, F., Otero, J., Lapazaran, J., & Błaszczyk, M. (2015). Estimate of the total volume of Svalbard glaciers, and their potential contribution to sea-level rise, using new regionally based scaling relationships. *Journal of Glaciology*, 51(225), 29–41. <https://doi.org/10.3189/2015JoG14J159>
- Martín-Español, A., Vasilenko, E. V., Navarro, F., Otero, J., Lapazaran, J., Lavrentiev, I., et al. (2013). Radio-echo sounding and ice volume estimates of western Nordenskiöld land glaciers, Svalbard. *Annals of Glaciology*, 54, 211–217. <https://doi.org/10.3189/2013AoG64A109>
- Melvold, K., & Schuler, T. (2008). *Mapping of subglacial topography using GPR for determining subglacial hydraulic conditions*. In: *Applied geophysics in periglacial environments* [eds. Hauck and Kneisel]. Cambridge, United Kingdom and New York, USA: University Press.
- Melvold, K., Schuler, T., & Lappegard, G. (2003). Ground-water intrusions in a mine beneath Høganesbreen, Svalbard: Assessing the possibility of evacuating water subglacially. *Annals of Glaciology*, 37, 269–274.
- Moholdt, G., Hagen, J., Eiken, T., & Schuler, T. (2010a). Geometric changes and mass balance of the Austfonna ice cap, Svalbard. *The Cryosphere*, 4(1), 21–34. <https://doi.org/10.5194/tc-4-21-2010>
- Moholdt, G., & Käbb, A. (2012). A new DEM of the Austfonna ice cap by combining differential SAR interferometry with ICESat laser altimetry. *Physical Review*, 31(18460). <https://doi.org/10.3402/polar.v31i0.18460>
- Moholdt, G., Nuth, C., Hagen, J., & Kohler, J. (2010b). Recent elevation changes of Svalbard glaciers derived from ICESat laser altimetry. *Remote Sensing of Environment*, 114(11), 2756–2767. <https://doi.org/10.1016/j.rse.2010.06.008>
- Morland, L. (1986). Unconfined Ice-Shelf Flow. In C. J. Van der Veen & J. Oerlemans (Eds.), *Dynamics of the West Antarctic ice sheet. Glaciology and Quaternary Geology* (Vol 4). Dordrecht, Netherlands: Springer.
- Morlighem, M., Rignot, E., Seroussi, H. H., Larour, E., Ben Dhia, H., & Aubry, D. (2011). A mass conservation approach for mapping glacier ice thickness. *Geophysical Research Letters*, 38, L19503. <https://doi.org/10.1029/2011GL048659>
- Navarro, F., Glazovsky, A., Macheret, Y., Vasilenko, E., Corcuera, M., & Cuadrado, M. (2005). Ice-volume changes (1936-1990) and structure of Aldegondabreen, Spitsbergen. *Annals of Glaciology*, 42, 158–162.
- Navarro, F., Martín-Español, A., Lapazaran, J., Grabiec, M., Otero, J., Vasilenko, E., & Puczek, D. (2014). Ice volume estimates from ground-penetrating radar surveys, Wedel Jarlsberg land glaciers, Svalbard. *Arctic, Antarctic, and Alpine Research*, 46(2), 394–406. <https://doi.org/10.1657/1938-4246-46.2.394>
- Navarro, F., Möller, R., Vasilenko, E., Martín-Español, A., Finkelnburg, R., & Möller, M. (2015). Ice thickness distribution and hydrothermal structure of Elfenbein and Sveigbreen, eastern Spitsbergen, Svalbard. *Journal of Glaciology*, 61, 1015–1018. <https://doi.org/10.3189/2015JoG15J141>
- Noël, B., van de Berg, W., Machguth, H., Lhermitte, S., Howat, I., Fettweis, X., & van den Broeke, M. (2016). A daily, 1 km resolution data set of downscaled Greenland ice sheet surface mass balance (1958–2015). *The Cryosphere*, 10(5), 2361–2377. <https://doi.org/10.5194/tc-10-2361-2016>
- Norwegian Polar Institute (2014). Terrenmodell Svalbard (S0 Terrenmodell). <https://doi.org/10.21334/npolar.2014.dce53a47>
- Nuth, C., Kohler, J., König, M., von Deschwanden, A., Hagen, J., Käbb, A., et al. (2013). Decadal changes from a multi-temporal glacier inventory of Svalbard. *The Cryosphere*, 7(5), 1603–1621. <https://doi.org/10.5194/tc-7-1603-2013>
- Nuth, C., Moholdt, G., Kohler, J., Hagen, J., & Käbb, A. (2010). Svalbard glacier elevation changes and contribution to sea level rise. *Journal of Geophysical Research*, 115, f01008. <https://doi.org/10.1029/2008JF001223>
- Ohmura, A. (2004). *Cryosphere during the twentieth century*, Geophysical Monograph 150, vol. 19, pp. 239–257. Washington, DC: IUGG. <https://doi.org/10.1029/150GM19>
- Pettersson, R., Christoffersen, P., Dowdeswell, J., Pohjola, V., Hubbard, A., & Strozzi, T. (2011). Ice thickness and basal conditions of Vestfonna ice cap, eastern Svalbard. *Geografiska Annaler: Series A, Physical Geography*, 93, 311–322. <https://doi.org/10.1111/j.1468-0459.2011.00438.x>

- Pinglot, J., Hagen, J., Melvold, K., Eiken, T., & Vincent, C. (2001). A mean net accumulation pattern derived from radioactive layers and radar soundings on Austfonna, Nordaustlandet, Svalbard. *Journal of Glaciology*, 47(159), 555–566. <https://doi.org/10.3189/172756501781831800>
- Pinglot, J., Pourchet, M., Lefauconnier, B., Hagen, J., Isaksson, E., Vaikmae, R., & Kamiyama, K. (1999). Accumulation in Svalbard glaciers deduced from ice cores with nuclear tests and Chernobyl reference layers. *Polar Research*, 18(2), 315–321. <https://doi.org/10.1111/j.1751-8369.1999.tb00309.x>
- RGI Consortium (2017). *Randolph Glacier Inventory - A Dataset of Global Glacier Outlines: Version 6.0: Technical Report*. Colorado, USA: Global Land Ice Measurements from Space. <https://doi.org/10.7265/N5-RGI-60> Digital Media.
- Radić, V., Bliss, A., Beedlow, A., Hock, R., & Cogley, E. M. J. (2014). Regional and global projections of twenty-first century glacier mass changes in response to climate scenarios from global climate models. *Climate Dynamics*, 42(1), 37–58. <https://doi.org/10.1007/s00382-013-1719-7>
- Radić, V., & Hock, R. (2010). Regional and global volumes of glaciers derived from statistical upscaling of glacier inventory data. *Journal of Geophysical Research*, 115, F01010. <https://doi.org/10.1029/2009JF001373>
- Saintenoy, A., Friedt, J., Booth, A., Tolle, F., Bernard, E., Laffly, D., et al. (2013). Deriving ice thickness, glacier volume and bedrock morphology of Austre Lovénbreen (Svalbard) using GPR. *Near Surface Geophysics*, 11, 253–261. <https://doi.org/10.3997/1873-0604.2012040>
- Schuler, T., Melvold, K., Hagen, J., & Hock, R. (2005). Assessing the future evolution of meltwater intrusions into a mine below Gruefonna, Svalbard. *Annals of Glaciology*, 42, 262–268.
- Schutz, B., Zwally, H., Shuman, C., Hancock, D., & DiMarzio, J. (2005). Overview of the ICESat mission. *Geophysical Research Letters*, 32, L21S01. <https://doi.org/10.1029/2005GL024009>
- Seehaus, T., Marinsek, S., Skvarca, P., van Wessem, J., Reijmer, C., Seco, J., & Braun, M. (2016). Antarctic Peninsula, to ice shelf breakup derived from multi-mission remote sensing time series. *Frontiers in Earth Science*, 4, 66. <https://doi.org/10.3389/feart.2016.00066>
- Strozzi, T., Luckman, A., Murray, T., Wegmüller, U., & Werner, C. L. (2002). Glacier motion estimation using SAR offset-tracking procedures. *IEEE Transactions on Geoscience and Remote Sensing*, 40(11), 2384–2391. <https://doi.org/10.1109/TGRS.2002.805079>
- van Pelt, W., Oerlemans, J., Reijmer, C., Pettersson, R., Pohjola, V., Isaksson, E., & Divine, D. (2013). An iterative inverse method to estimate basal topography and initialize ice flow models. *The Cryosphere*, 7, 987–1006. <https://doi.org/10.5194/tc-7-987-2013>
- Vasilenko, E., Navarro, F., Dunse, T., Eiken, T., Hagen, J., & Moholdt, G. (2009). New low-frequency radio-echo soundings of Austfonna ice cap, Svalbard. In A. P. Ahlström & M. Sharp (Eds.), *Extended Abstracts, Workshop and GLACIODYN (IPY) Meeting* (pp. 64–67). 16–19 February 2009, Kananaskis (Canada).
- Vaughan, D., Comiso, J., Allison, I., Carrasco, J., Kaser, G., Kwok, R., et al. (2013). *Observations: Cryosphere, climate change, 2013, the physical science basis. Contribution of working group I to the Fifth Assessment Report of the Intergovernmental Panel on Climate Change*. Cambridge, United Kingdom and New York, NY: Cambridge University Press.
- Wingham, D., Francis, C., Baker, S., Bouzinac, C., Brockley, D., Cullen, R., et al. (2006). CryoSat: A mission to determine the fluctuations in Earth's land and marine ice fields. *Natural Hazards and Oceanographic Processes from Satellite Data*, 37, 841–871.
- Wouters, B., Chambers, D., & Schrama, E. (2008). GRACE observes small-scale mass loss in Greenland. *Geophysical Research Letters*, 35, L20501. <https://doi.org/10.1029/2008GL034816>
- Zagorodnov, V., & Arkhipov, S. (1990). Studies of structure, composition and temperature regime of sheet glaciers of Svalbard and Severnaya Zemlya: Methods and outcomes. *Bulletin of Glacier Research*, 8, 19–28.
- Zagorodnov, V., & Samoilov, O. (1982). Internal structure of Spitsbergen glaciers. *Data of Glaciological Studies*, 44, 58–64.
- Zagorodnov, V., & Zotikov, I. (1981). Capillary channels in glaciers. *Data of Glaciological Studies*, 41, 200–202.